

---

# Volatile Network as a Simple Memory Model

**Rainer Willi Schulze**

Faculty of Computer Science, Dresden University of Technology, Dresden, Germany

**Email address:**

[rainer.schulze@tu-dresden.de](mailto:rainer.schulze@tu-dresden.de)

**To cite this article:**

Rainer Willi Schulze. Volatile Network as a Simple Memory Model. *American Journal of Mathematical and Computer Modelling*. Vol. 8, No. 1, 2023, pp. 6-16. doi: 10.11648/j.ajmcm.20230801.12

**Received:** February 10, 2023; **Accepted:** February 27, 2023; **Published:** May 22, 2023

---

**Abstract:** Technical information systems, from PCs to supercomputers, are characterized over time by ever-increasing storage capacities, while biological systems are permanently characterized by their trainable memory abilities. Although both systems are not comparable with each other, because they are based on different phenomena, the existing efficiency of biological systems offers a constant borrowing for the further development of technical systems. For this purpose, it is necessary to develop technical equivalence models. The following considerations aim to reproduce the factually limitless abilities of biological systems to store memory content as a result of the plasticity of neuronal populations. The difference between technical and biological systems becomes particularly clear under this aspect: while the development of technical systems aims to permanently increase the existing storage capacity, biological systems are based on independently separating relevant from irrelevant information and, moreover, permanently reorienting existing memory structures, called plasticity. Accordingly, the transmitter flow between the neurons constantly changes in direction and intensity. A network with a transient topology that is marginally able to model a memory-capable neuronal population characterized by a permanent loss of neuronal contact points is proposed for discussion. Such a loss permanently changes the direction and intensity of the transmitter flow between the neurons. Another focus of the topic is the question of how different stimuli, meaning optical, acoustic, tactile, etc., can become one and the same memory description of a neuron population. Here it is assumed that a pre-processing takes place in the biological system in the form of a functional transformation, the result of which is a neutral basis for representing the information. Although such an assumption seems to be highly speculative, a discussion of it would contribute to answering the question of which physiological mechanisms have to be taken into account to explain memory phenomena, reproduced in a model.

**Keywords:** Engrams, Memory Structure, Observation Space, Memory Stimulator, Degeneration, Fokker-Planck Equation, Jacobian Matrix

---

## 1. Introduction

Architectures of technical and biological systems are fundamentally not comparable with each other, neither in their structure nor in their function. Nevertheless, a technical borrowing from biological model systems is of interest, although a formal transfer of neuronal into technical structures has not proven to be expedient. Although the discovery of gestalt neurons (*Hubbel* and *Wiesel*) in the cat brain in the second half of the last century was important for the development of artificial neural networks, it soon turned out that in a neuron population a single neuron has no singular significance [1]. The assumption of a so-called grandmother neuron, which reacts singularly to an excitation

in lateral independence, is irrelevant. Rather, the interest in brain research has developed in the direction of finding out which track (: engram) neuronal excitation takes in a population in space and time. Richard Semon (a member of the *Leopoldina*) coined the term engram as the permanent memory entry and thus explained the inheritance of properties [2]. In this context, it is of interest how engrams permeate each other, how they can self-organize from dysfunctional to functional areas of the brain (: plasticity). These effects inspired and still inspire the development of technical systems for information processing, for example those with associatively organized storage mechanisms.

Equally interesting are the different signal carriers in the case of a technical borrowing from biological model systems. One and the same system not only picks up different signal

carriers in parallel, but also processes them together in order to subsequently store them in one and the same neuron population. This applies, for example, to the overall impression of space and acoustics in a concert hall and in an opera house. Due to the complex perception of space and acoustics, a memory entry is formed that differs significantly from the singular perception of the acoustics [3].

The question is: Which signal carriers represent a lasting complex impression in one and the same biological system? Brain researchers are responsible for answering such a question. In the following, the question of whether the original memory content received via a certain channel is subject to a functional transformation before being stored in a neuron population is attempted, which offers a common basis for all channels [4].

A next question is: How does the biological system independently organize the whereabouts or loss of recorded memory content. In the event that content is of negligible relevance, it will be deleted, formulated in the technical terminus, otherwise it will be preserved. To simulate this phenomenon, a technical arrangement is presented, consisting of a network with volatile topology and an integrated memory stimulator. Parameters are consistency rate  $\lambda$  and memory ability  $\eta$ . Both parameters together measure the memory loss along the trace of an engram, equated along a time axis. No matter how intense the ability to remember, any memory content is only temporary and is lost over time.

## 2. Storage of Memory Contents

A nervous system represents a higher-dimensional action space, consisting of a myriad of locations for accommodating neurons, which are linked to one another via synapses. Sperry, Nobel Prize winner for medicine, held the view that humans are born with an excess of synaptic connections, but over time they degrade in a problem-oriented manner in order to develop over time their individual, unmistakable nature [5]. According to this, neural connections only exist temporarily, which raises the following questions from a system-theoretical point of view:

- 1) What transformation exists between the arousal environment and the structure of the nervous system, derived from this the question:
- 2) Who or what determines the coupling weights of the synapses, closely related question:
- 3) What breakdown processes take place in the nervous system?

Question (1) refers to the large number of qualitative and quantitative stimuli on the nervous system, their filtering and their entry into existing memory structures. Due to the plasticity of the nervous system, it can be expected that the topology of the nervous system will adapt to this complexity. Although a dedicated description of this with the help of systems theory would be interesting, for example to be able to distinguish between self-perception and external perception, it would contradict any capacity for tolerance.

However, such an ability should be indispensable for the coexistence of living systems.

Question (2) can be answered decisively. Existence and perception of stimuli are two different phenomena. Sensory organs such as the light-sensing cells in the visual system of vertebrates receive an optical pattern as a conglomerate of a multitude of complex light stimuli and convert them in detail into generator potentials for further processing in the downstream layers. Finally, the storage of the optical pattern in a memory structure is not true to the texture, that means isomorphic, but relational. It is not the local intensity distribution of the pattern that is stored in a memory structure, but rather the relationships between the locations of the intensities in the pattern, referred to as coupling weights.

These entries in the memory structure are autonomous and volatile in order to guarantee an orderly filing of memory content within the memory structure over time.

Question (3) relates to gerontological and pathological changes in the nervous system. As a result, the memory structure increasingly loses its ability to store memory content, caused, for example, by plaque formation on the membrane of postsynaptic neurons, but also by tauopathy inside the neuron [6, 7, 8].

### 2.1. Interactions Between the Points in Space

Given is a population of a large number of neurons coupled to each other via synapses, modeled as a traffic field of nodes that interact with each other via an embossed coupling structure. The interactions of the nodes are to be simulated. A marked coupling flow circulates between them, controlled by an associated reference field (Figure 1).

From an abstract point of view, the traffic field exists as an n-dimensional accommodation  ${}^{(m)}\mathbb{R}^{(n)}$  of m space points P from  $P = \{P_1, \dots, P_m\}$  in an n-dimensional discrete Action space  $\mathbb{Z}_{\lambda>0}^n$ , i.e.  ${}^{(m)}\mathbb{R}^{(n)}: P \rightarrow \mathbb{Z}_{\lambda>0}^n$ , where  $\xi$  n-dimensional coordinate tuple of P in  $\mathbb{Z}_{\lambda>0}^n$ .

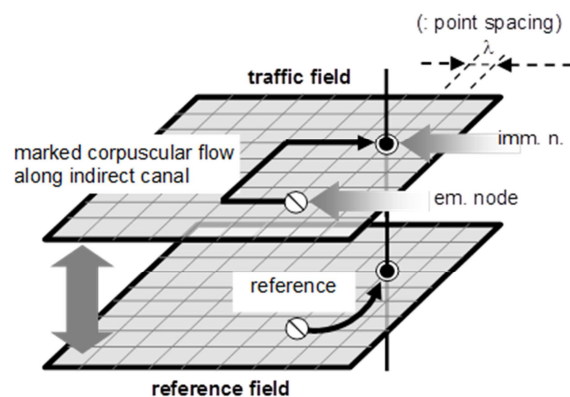


Figure 1. Topology of a sandwich architecture, consisting of traffic and processor field.

A marked corpuscle flow is driven across the traffic field, the orientation of which is determined both by the topology between the resources and by the reference distribution between them.

The dynamics of the traffic field is observed at discrete points in time  $\tau$  on a *discrete time scale*  $T_{\Delta\tau}$  in a n-dim. *discrete time-based observation space*  $\mathbb{B}_{\lambda>0}^n = \mathbb{Z}_{\lambda>0}^n \times T_{\Delta\tau}$ .

$$\mathbb{B}_{\lambda>0}^n = \{X(j_1; \tau_1), \dots, X(j_N; \tau_T)\}$$

At the initial point in time  $\tau_0$ , an inhomogeneously distributed concentration pattern may act on all m spatial points P from P, referred to as the excitation pattern  $X = \{X_1, \dots, X_j, \dots, X_m\}$  of the traffic field. Diffusion is a concentration equalization through undirected random movements [14]. In the present case, it is a question of controlled referencing by a reference field. The necessary references  $A(P', P; \tau)$  from P to P' at time  $\tau$  are to be calculated. The time invariance  $A(P', P; \tau)$  granted here guarantees the maintenance of the inner dynamics of the action space during the balancing process.

The interactions manifest themselves in the permanent referencing of emitting through emitting nodes, as a result of which the status of the nodes and thus their weighting in relation to one another changes constantly. Under certain circumstances, and this is the actual goal of the procedure, some nodes in the traffic field lose their relevance and must therefore be relegated. Likewise, all incoming and outgoing connections are eliminated. The aim is to achieve a maximum number of connection extractions in this way.

The process is modeled taking into account the time invariance in the n-dim. discrete action space  $\mathbb{Z}_{\lambda>0}^n$ , the simulation on the other hand in n-dim. Vector space  $\mathbb{R}^n$ .

## 2.2. Referencing Between the Spatial Points

Multidimensionality of a discrete space means splitting the space into a corresponding number of coordinate axes  $\xi$ . In  $\mathbb{Z}_{\lambda>0}^n$ , the function values  $X(\xi)$  in the n-tuples  $\xi = (\xi_1, \dots, \xi_n)$  are interpolation points of a function f in a continuous vector space R. In fact, the metric distance is the Interpolation points in relation to each other for the formation of the discrete Fourier transform  $\mathfrak{F}\{X(\xi); k\}$  as a discrete spectral function A(k) of X( $\xi$ ) are of no importance, as a result of which a 1-dim vector space  $\mathbb{R}^1$  can suffice for the formation of  $\mathfrak{F}$ . Each n-tuple  $\xi = (\xi_1, \dots, \xi_n)$  in  $\mathbb{Z}_{\lambda>0}^n$  is assigned an argument x from f(x) in  $\mathbb{R}^1$ .

Suppose  $f(x) = f(x \pm nL)$ , then

$$\xi \rightarrow x: \mathfrak{F}\{X(\xi); k\} = A(k) = \frac{1}{2N-1} \sum_{x=1-N}^{N-1} f(x) \exp(-i\omega_0 xk)$$

Under  $\omega_0 = \frac{2\pi}{2N-1}$ ,  $i = \sqrt{-1}$ ,  $L=2N$ ,  $k = 1 - N, \dots, 0, \dots, N-1$

Suppose  $f(x) = f(-x)$ , then

$$A(k) = \frac{2}{2N-1} \sum_{x=0}^{N-1} f(x) \cos(\omega_0 xk) - X_0 \text{ with } X_0 = X(x=0)$$

and reciprocally unique

$$f(x) = f(-x) = \frac{2}{2N-1} \sum_{x=0}^{N-1} A(k) \cos(\omega_0 xk) - A_0$$

With

$$A_0 = A(k=0) \quad (1)$$

It reads (2-1) in matrix representation  $\frac{2}{2N-1} W_{X \rightarrow A} \cdot f = a$  and  $W_{A \rightarrow X} \cdot a = f$

Under  $f = (f_0, f_1, \dots, f_x, \dots, f_{N-1})$  mit  $f_x = f(x)$  sowie  $a = (a_0, a_1, \dots, a_k, \dots, a_{N-1})$  mit  $a_k = A(k)$

It is  $W_{X \rightarrow A} = \parallel^k w_x \parallel_{0 \dots N-1; 0 \dots N-1}$  under

$${}^k w_x = \begin{cases} \frac{1}{2} \text{ für } x = 0 \\ \cos(\omega_0 xk) \text{ für } x > 0 \end{cases}$$

And  $W_{A \rightarrow X} = \parallel^x w_k \parallel_{0 \dots N-1; 0 \dots N-1}$  under

$${}^x w_k = \begin{cases} \frac{1}{2} \text{ für } k = 0 \\ \cos(\omega_0 xk) \text{ für } k > 0 \end{cases}$$

W is a column and row ordered coefficient matrix for performing the Discrete Fourier Transform.  $W_{A \rightarrow X}$  generates the spectra  $a_0, \dots, a_{N-1}$  weighted with the corresponding Fourier coefficients  $\cos(\omega_0 \cdot x \cdot k_{0, \dots, N-1})$  the function value f(x) at the point x into arousal pattern.

$$f(x) = 2 \sum_{k=0}^{N-1} A(k) \cos(\omega_0 xk) - A_0 \text{ with } X_0 = X(x=0) \quad (2)$$

In a figurative sense, the architecture of (2-2) describes the interaction of the traffic and reference fields. If the elements of the traffic field do not exist in the original but in a previously determined spectral range, the sum of the references of all spatial points P to a spatial point P' represents its function value f in the original [9].

All references between the spatial points, accordingly all interactions between the neurons of a population, are positively signed. Accordingly, the coefficients  $A(k) \cos(\omega_0 xk)$  in (2-2) are to be normalized.

$$\text{Let } \mathbb{Y} = \{A(k) \cos(\omega_0 xk) \mid x(k) = 0, \dots, N-1\}$$

set of all Fourier coefficients,

$$\text{then } 0 \leq {}^x y_k = 1 + \frac{A(k) \cos(\omega_0 xk)}{\inf \mathbb{Y}} \quad (3)$$

is positively signed reference from  $P_k$  to  ${}^x P$ , the space points from P.

## 2.3. Topology Reduction

In biology, the term "evolution" stands for the increase in resilient properties of a biological system or for overcoming inhibiting properties. At the same time, changes of state also take place in physical systems. Change energy is consumed for this. If this energy is spent inside a system and no external supply is supplied, it retains its assumed state. A capacitor, for example, is able to store energy by separating charges. This requires internal energy, mediated by an applied voltage. The capacitor has reached its capacity limit, its change energy is exhausted, and there is no longer any charge separation. Its condition is preserved [10].

With regard to the energy supply and capacity limit of physical systems, a borrowing can be used to optimize the topology of neuronal memory structures. Memory structures, so-called engrams, are formed, they penetrate each other, interact with each other and thus process information. Frequencies of synaptic connections taken thereby reflect their relevance for storing memory content.

From a physical point of view, the formation of engrams is an energy-consuming process, supported, among other things, by the consumption of glucose, the more intense the more frequently a synaptic connection is used. It seems plausible to dissolve less frequently used connections in order to gain energy for more frequently used ones. The reduction algorithm in a discrete action space  $\mathbb{Z}_{\lambda>0}^n$  for modeling and simulating the ability to remember is based on this assumption [11].

If all nodes continue to exist, the topology reduction in the discrete action space is carried out solely by a conditional removal of existing arcs between them.

First, the most weakly referenced node of all arcs is declared as one to be removed.

Should the arc so removed result in either loss of mutual reachability between all nodes, indicated by a minimum matrix  $M$ , or loss of corpuscular flow balance between nodes, the removal is annulled. Subsequently, the second weakest referenced of all arcs is declared as one to be removed, and so on.

The reduction ends when no more arcs can be found that fulfill requirement 2.

Between the nodes of the traffic field (Figure 1), corpuscular flows circulate, the thicknesses of which change as arcs are removed, so they have to be recalculated after each removal.

According to its references, each node emits and emits its contribution to all corpuscle flows in the traffic field, consuming time. The transfer times between the nodes are related to their references. Balance exists when the time consumption for corpuscle immission and emission correspond to each other. Each node  $P$  emits corpuscle streams in a distribution time and emits incoming corpuscle streams in a collection time in the time shadow, parameterized by

- 1) Preparation time  $c$  for the transfer of a corpuscle massif along an arc,
- 2) Transfer time  $q$  of a corpuscle along an arc, depending on
- 3) Velocity  $v$  of the corpuscle transfer and actually taken
- 4) Path length  $s$  of a corpuscle.

The demand for balance in relation to the transfer time between the nodes results in a linear system of equations  $K \cdot \overset{\otimes}{n} = b$  for the calculation of balanced sizes of circulating corpuscle flows.

#### 2.4. Memory Stimulator

From a system-theoretical point of view, memory is understood to mean the acquisition and maintenance of a state. Richard Semon (Member of the Leopoldina) explained the memory ability of a neuron population with the formation of a

memory trace (: engram). The Freiburg scientists *M. Bartos* and *Th. Hainmüller* [12] support this phenomenon and suspect that memory formation in the brain is accompanied by a change in synaptic connection strengths between inhibitory and excitatory nerve cells (: *synaptic plasticity*).

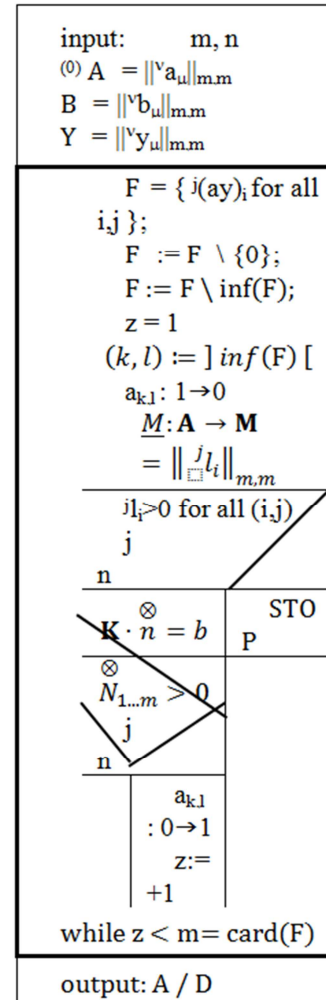


**Figure 2.** Structogram of the topology reduction: The elements of the adjacency and reference matrix are accommodated in a linearly ordered set  $F$  with the relation  $<$ . Outside of the 0 elements, the infimum of  $F$  and its address or indices are determined. Subsequently, the corresponding element  $a$  of the adjacency matrix  $A$  is converted from 1 to 0 and it is determined whether the accessibility of the spatial points  $P$  to each other has been retained. Then there is a solution of the system of equations  $K \cdot \overset{\otimes}{n} = b$  for the sizes of the corpuscle emissions  $N_{1...m}$  from the space points  $P_{1...m}$ . In the case of only positively signed solutions, the annulment of  $a$  is retained, otherwise the return  $a:0 \rightarrow 1$  takes place. The element corresponding to the return is taken from the set  $F$  and the next infimum of  $F$  is then determined. The topology reduction ends when, after a transfer from  $a:1 \rightarrow 0$  the spatial points  $P$  is no longer accessible to one another or no positively signed element can be found in the set of  $m$  thicknesses  $\overset{\otimes}{N}$ .

In this context, it is of interest how engrams permeate each other, how they can self-organize from dysfunctional to functional areas of the brain (: plasticity). Neural connections only exist temporarily, and the following is of interest:

What is the transformation between the arousal environment and the structure of the nervous system,

derived from this the question:

Who or what determines the coupling weights of the synapses,

closely related question:

What breakdown processes take place in the nervous system?

Conditional retention and loss of memory content is modeled in Figure 3.

Not every neuron in the population is connected to every other neuron via synapses, an adjacency matrix  $A$  models the concrete topology. In view of Sperry's assumption that humans are born with an excess of synaptic connections, the adjacency matrix is fully occupied in the initial state, excluding a connection with oneself.

Synapses change their connection strength; the presynaptic release of transmitter molecules can vary. Catalysts (: *enzymes*) influence their transfer across the synaptic cleft. They are temperature-dependent, their effect in the organism is linked to the ambient temperature. The receptors of the postsynaptic membrane bind the transferred molecules.

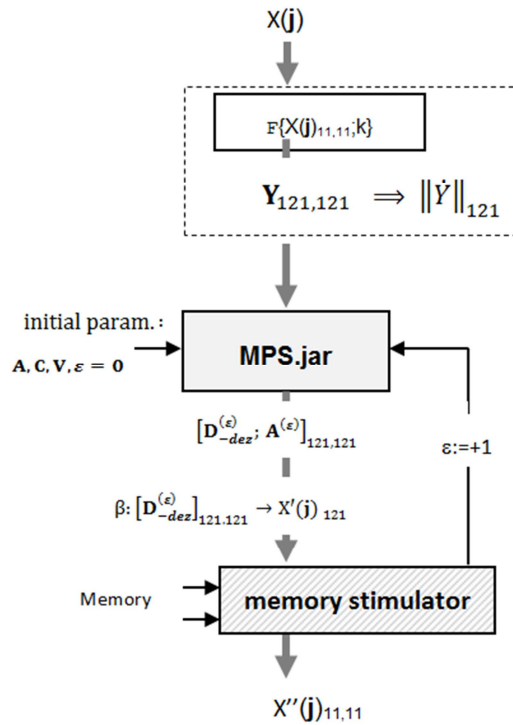


**Figure 3.** A reference matrix  $Y$  results from the Fourier transform of an excitation pattern  $X(j)$ . The program *MPS.jar* constantly simulates the topology reduction of the population. A resulting memory loss can be compensated for within limits by a memory simulator.

For the duration of their connection, sodium channels open for the influx of positively charged sodium ions into the interior of the postsynaptic neuron. In addition, the connection strength of a synapse is related to the frequency of its use. In the simulation model [8], a synapse is characterized by its transfer speed for transmitter molecules, parameterized by the elements  $v$  of a speed matrix  $V$ , but also by the relative frequencies  $y$  as elements of a reference matrix  $Y$ .

After each influx of  $NA^+$  ions, a neuron goes through a refractory period - a time interval in which no new transmitter molecules can be released. This property takes into account a refractory matrix  $C$  whose elements  $c$  are called refractory periods. From a physical point of view, this is how a neuron protects itself from energetic exhaustion.

The simulation model [13] for retention and loss of memory content exists in a discrete observation space. All components, here the neurons of the population, exist at a discrete distance from each other, either directly or only indirectly coupled. The distances change with the structuring of the population, that means change permanently with the problem-oriented removal of direct connections. The remaining path lengths between them are the elements  $s$  of a taximetrics' path length matrix  $S$ . If all neurons were directly connected,  $S$  would be a Euclidean distance matrix.

In summary, the simulation model for simulating transient activities in a neuron population consists of the following

Parameter set:

$A$  (: *adjacency matrix* for the topology of the neuron population),

$C$  (: *refractory matrix* for the passive time of the neurons),

$V$  (: *velocity matrix* for excitation transfer along a direct connection),

$S$  (: *Matrix of taximetrics' path lengths* in the initial state  $\varepsilon=0$ )

with  $\varepsilon$  as index for the current reduction step in the model (: reduction step).

Due to the permanent loss of synaptic connections, the power of circulating transmitter flows in the population changes constantly. In the simulation model, this effect is simulated by a permanently changing thickness of circulating corpuscle massifs. It is  $\mu d_v^{(\varepsilon)}$  the thickness of a corpuscular massif emitted in  $P_v$  and immitted by  $^{\mu}P$  in reduction level  $\varepsilon$ .

Neuronal status  $S$ : The simulation network for the neuron population loses its consistency  $\lambda$  with an increasing number  $\varepsilon$  of reduction steps (: number of direct couplings), and accordingly also the ability to reconstruct an initial excitation  $X(j)$ . This is counteracted by the effort required for memory training, parameterized by the ability to remember  $\eta$ . Both parameters  $\lambda$  and  $\eta$  determine the neuronal status  $S(\varepsilon)$  of the network in the reduction step  $\varepsilon$  for the simulation of the neuron population.

$$S(\varepsilon) = [(1 - \eta)\lambda]^{(\varepsilon)}$$

**Consistency rate  $\lambda$ :** Ratio of the number of existing direct connections to the number potentially possible connections in a network.

**Memory rate  $\eta$ :** Rate of recognition of patterns from an ensemble initial arousal pattern,  $0 < \eta < 1.0$ .

A distinction is made between imprinting and memory. The imprinting of a network means the initial excitation pattern  $X(j)$ . It loses significance as a result of the ongoing reduction in direct connections between the nodes. The imprint that still exists in a reduction stage  $\varepsilon$  depends on the existing ability to remember  $\eta$ . The memory stimulator

relativizes the interplay between loss of significance and imprinting. Its task is to filter out the smoothing of the initial excitation pattern  $X(j)$  according to the neuronal status  $S$  by means of selectors  $f$ . A distinction is made between the selectors  $f_U$  for the area around the embossing and  $f_K$  along the embossing.

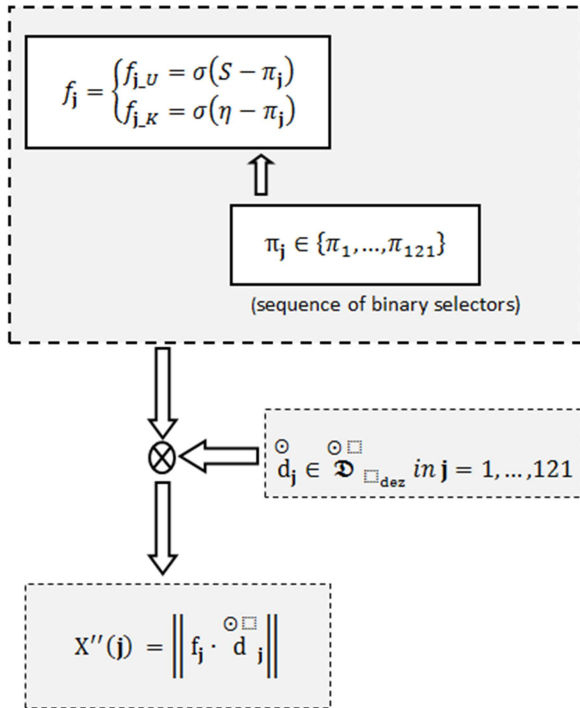


**Figure 4.** Architecture of a memory stimulator. A sequence of binary selectors  $f$ , developed from the correction factors  $\pi$  related to the neuronal state  $S$ , is multiplied by the normalized elements  $d$  of the corpuscle matrix  $D$ , resulting in the elements  $x''$  of a secondary excitation distribution  $X''$  taken in the reduction step  $\varepsilon$ . In detail,  $f_{j,K}$  denotes a selector along the excitation contour and  $f_{j,U}$  in the vicinity.

Multiplying  $d_j^{(\varepsilon)}$  by the correction factor  $f_j^{(\varepsilon)}$  gives the element  $\mu_{x''_v}^{(\varepsilon)}$  of the secondary excitation distribution  $X''(j)$  - the output from the memory stimulator (Figure 4).

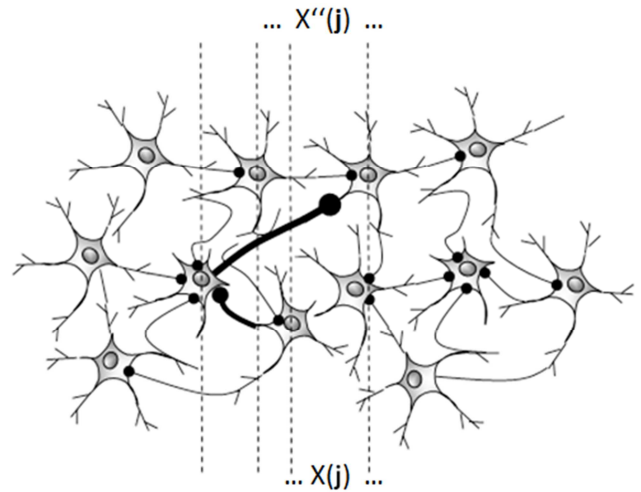
$$\mu_{x''_v}^{(\varepsilon)} = \mu_{f_v}^{(\varepsilon)} \cdot \mu_{d_v}^{(\varepsilon)} = \left[ f \cdot d \right]_v^{(\varepsilon)} \in X''(j)$$

The correlation  $r(X(j); X''(j))$  describes the quality of the memory stimulator.

### 3. Example

In order to clarify properties, the following explanations use both the planar representation of locations as a 2-tuple  $(j_1, j_2)$  and  $(k_1, k_2)$  in  $1 \dots 11$  and a linear representation as a 1-tuple  $(j)$  in the following explanation and  $(k)$  given in  $1 \dots 121$ .

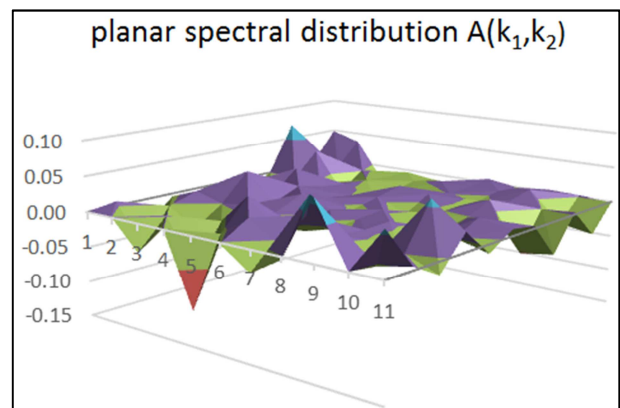
A neuron population (Figure 5) is to be modeled and simulated by a network with a volatile topology. The discrete distance between the neurons is measured as  $d$ , their coupling intensities are simulated by the relative reference frequencies  $y$ .



**Figure 5.** Isometric reconstruction: Simulation of the reconstruction  $X''(j) = X''(j_{1..N})$  from the initial excitation  $X(j)$  based on remaining direct connections with the connection strength  $y$ .

Figure 5 shows a section of a neuron population in which the initial excitation pattern  $X(j)$  is entered and subsequently smoothed out by the abolition of synaptic connections to  $X''(j)$ . The effect of such a smoothing can be determined by the dedicated distribution of the transmitter densities on the membrane surfaces of the neurons as well as the local flux density of transmitter currents between the neurons. This process is modeled by the volatile network described above, where the corpuscle density in the nodes of the network corresponds to the transmitter density in the population and the flux density of circulating corpuscle currents corresponds to the flux density of transmitter molecules. If there is consistency  $\lambda$  of the fleeting network, these densities are used as indicators for the characterization of memory retention of  $X(j)$ , parameterized by the memory depth  $\eta$ . It is plausible that the memory retention for one and the same excitation pattern in  $\eta$  is pronounced differently.

Figure 6 shows a discrete excitation pattern in a planar  $X(j_1, j_2)$  and linear representation over  $N=121$  spatial points, including the planar 2-dim.  $A(k_1, k_2)$  and linear 1-dim. Spectral distribution  $A(k)$  as a Fourier transform of  $X$ .



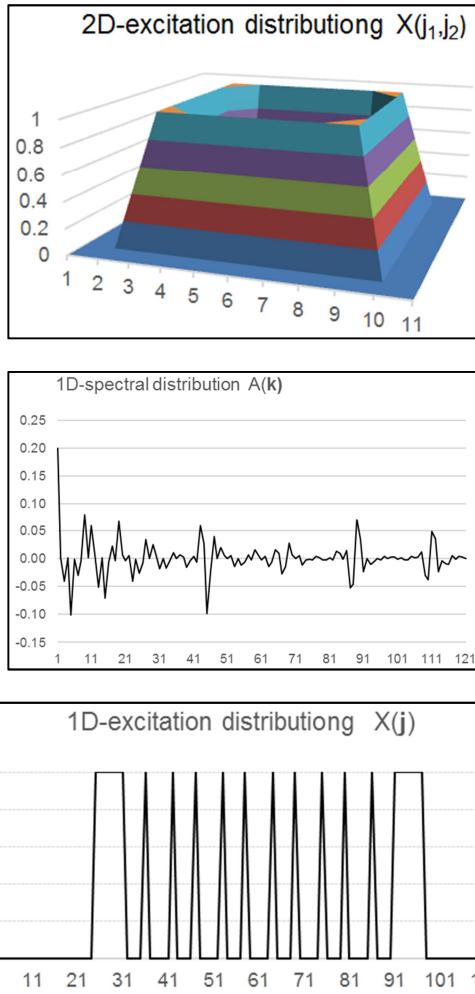


Figure 6. Planar and linear excitation distribution and the corresponding spectral distribution.

$$X'(j) \equiv X(j_1, j_2) = \mathfrak{F}^{-1}\{A((k_1, k_2)); (j_1, j_2)\}$$

*Inverse transformation* Under  $1 \leq k \leq 121$  with  $0.10 \leq A(k) \leq 0.2$ , the spectral distribution  $A(k)$  (Figure 6) is inverse transformed into the excitation pattern  $X(j)$  by means of Fourier inverse transformation without significant blurring of the contour (Figure 6). In this regard, there is still a correlation of 0.9 if the spectral frequency is narrowed to  $7 \leq k \leq 110$  and the amplitudes of the spectral function are discriminated in  $-0.10 \leq A(k) \rightarrow A'(k) \leq 0.18$ . On a planar level, Figure 7 shows the reduced spectral distribution  $A'(k_1, k_2)$  and its re-transform  $X'(j) = \mathfrak{F}^{-1}\{A'(k_1, k_2); (j_1, j_2)\}$ .

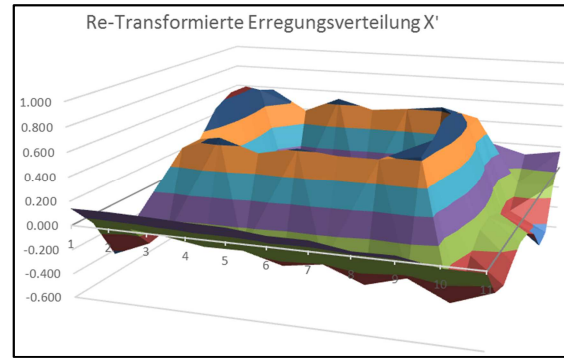
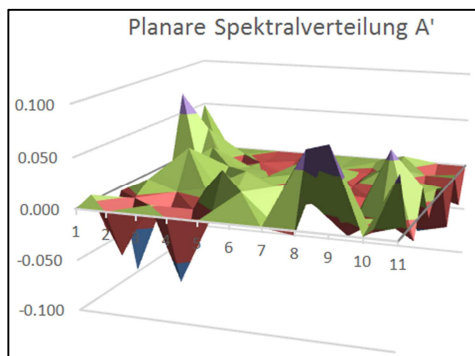


Figure 7. Reconstruction  $X'(j) = \mathfrak{F}^{-1}\{A'(k); j\}$  from the reduced spectral distribution  $A'(k)$ .

Band limitation and amplitude discrimination of the spectral distribution minimize the energy required to reconstruct an excitation pattern. It is more difficult to reconstruct topologically smooth excitation patterns in a network with volatile topology. It is characterized by a loss of direct connections, which corresponds to the loss of synaptic contact points in a population of neurons.

### 3.1. Simulation of Reconstruction Without a Memory Stimulator

The neuron population to be simulated drives a transmitter flow with a speed of 1cm/s, the refractory period of a neuron is  $c=10$  s. The development of the population is to be simulated in a fleeting topology. The transit times of the corpuscles from node to node in the network correspond to those from neuron to neuron in the population. The reconstruction of a registered excitation pattern shows a greater smoothing, the more synaptic contact points have been damaged in the meantime. The increasing reduction  $\epsilon := +1$  of direct connections in the network increases both the transit times between the nodes and the thicknesses of transferred corpuscle massifs.

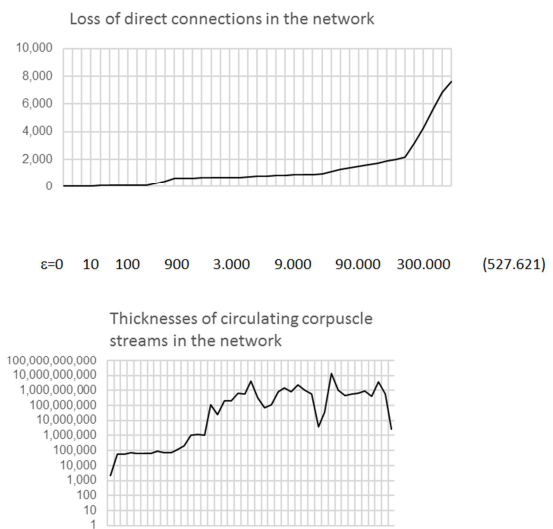


Figure 8. Resulting thicknesses of circulating corpuscle massifs with the loss of direct connections. The thickness of circulating corpuscle massifs plausibly increases with the progressive loss of direct connections - but not proportionally, shown for the reduction intervals in  $\epsilon \in 10^x \cdot \{0(10)100\}$  für  $x = 1, 2, \dots, 5$ .

Without a memory stimulator, the correlation between the excitation pattern  $X(j)$  and its reconstruction  $X''(j)$  falls to less than 15% with the removal of a single direct connection and falls to -5% with the removal of further connections (Figure 9). Without loss compensation, the volatile network would therefore no longer be able to reconstruct the entered excitation pattern  $X(j)$ .

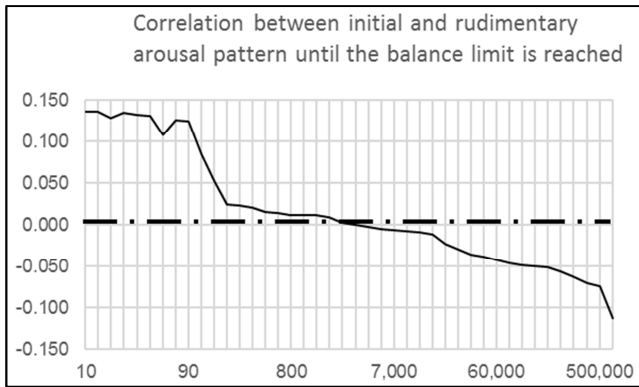


Figure 9. Correlation between initial and rudimentary excitation pattern without compensation for connection removals in the network.

In a network with an volatile and a memory stimulator, there are the following possibilities for a reconstruction of  $X(j)$  by the stimulator, albeit only approximately:

- 1) isometric reconstruction of the excitation patterns  $X(j)$  and  $X''(j)$ , indicated by the distribution of corpuscle densities over  $N$  spatial points  $P$  of the network;
- 2) Reconstruction of all vorticity strengths of the corpuscular flows circulating between the nodes of the network.

### 3.2. Isometric Reconstruction of the Excitation Pattern $X(j)$

Due to consistency  $\lambda$  and memory  $\eta$ , the stochastic distribution of the correlation coefficients  $r(X(j);X''(j))$  develops more and more differently as direct connections are progressively removed. The volatile network, parameterized with  $c=10$  s and  $v=1m/s$ , reaches its *balance limit* after  $\epsilon=527,621$  reduction steps. Figure 9 shows the course of the correlation coefficients  $\rho$  up to the reduction step  $\epsilon=10^5$  for different values  $\eta$ . The partial decrease of  $\rho$  for  $0.8 < \eta < 1,0$  to the local value 0.8 (Figure 10) at the point  $\epsilon=10^3$  is an exceptional situation, due to the stochastic character of the memory stimulator.

The curves shown in Figure 10 correspond to the statistical average over 24 sample sets of  $N=121$  random numbers each. In detail, Figure 10 shows the fluctuation range of the distribution of the correlation coefficients  $r$  over 24 sample sets in the event of a loss of approx.  $10^3$  direct connections depending on  $\eta$ .

Up to a loss of approx. 1.000 direct connections (Figure 11) an almost complete reconstruction of the initial excitation pattern takes place under  $\eta=0.9$ . Increasing loss of connections as well as declining memory  $\eta$  reduce this possibility. For example, a correlation coefficient greater than  $r=0.9$  with reduced memory  $\eta=0,8$  requires 13.750 direct connections to remain, which excludes exceeding

$\epsilon=300$  reduction steps. A higher-order correlation coefficient below a minimum requirement for memory ability  $\eta$  cannot be achieved with an isometric reconstruction of the excitation pattern  $X(j)$  and  $X''(j)$  using a memory stimulator, for example for  $\eta=0.5$  (Figure 10).

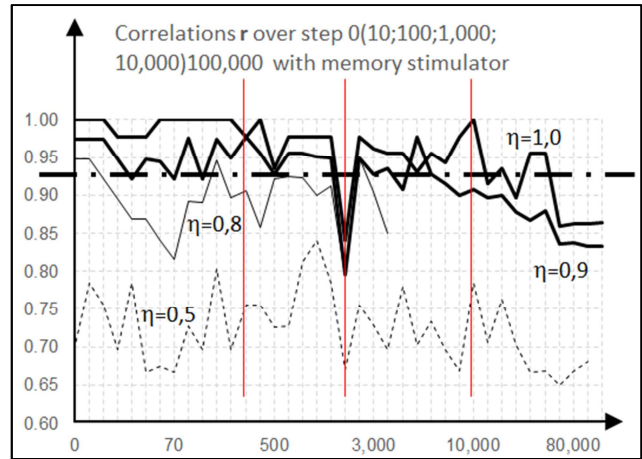


Figure 10. Fluctuation range of the correlation between  $X''(j)$  and  $X(j)$  with loss compensation by a memory stimulator; simulated for different memory abilities  $\eta$ .

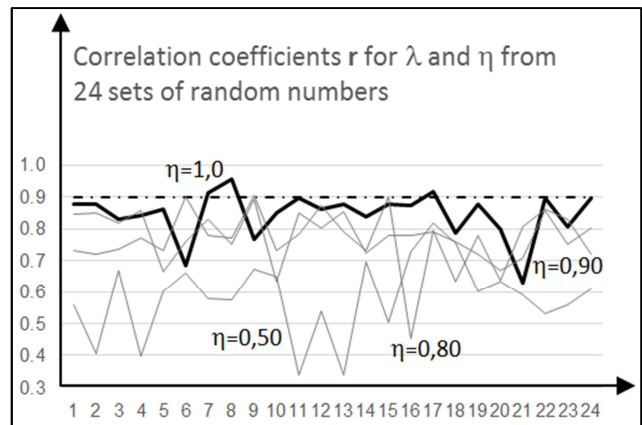


Figure 11. Variation range of the correlation  $\rho$  in  $\epsilon=10,000$  (consistency rate  $\lambda=0.935$ ) between  $X''(j)$  and  $X(j)$  over 24 samples for different memory abilities  $\eta=1.0(0.9; 0.8$  and  $0.5)$ .

Up to a loss of approx. 1.000 direct connections (Figure 11) an almost complete reconstruction of the initial excitation pattern takes place under  $\eta=0.9$ . Increasing loss of connections as well as declining memory  $\eta$  reduce this possibility. For example, a correlation coefficient greater than  $r=0,9$  with reduced memory  $\eta=0,8$  requires 13.750 direct connections to remain, which excludes exceeding  $\epsilon=300$  reduction steps. A higher-order correlation coefficient below a minimum requirement for memory ability  $\eta$  cannot be achieved with an isometric reconstruction of the excitation pattern  $X(j)$  and  $X''(j)$  using a memory stimulator, for example for  $\eta=0.5$  (Figure 10).

### 3.3. Reconstruction of the Vorticity of Circulating Corpuscular Flows

An alternative to the isometric reconstruction of the

excitation patterns is the reconstruction of the patterns on the basis of vortex strengths that interact with each other.

Each node in  $\mathbb{Z}_{\lambda>0}^{2<N}$  carries a corpuscular charge caused by the circulating corpuscular massif. In detail,  ${}^\mu d_v^{(\varepsilon)}$  is the corpuscle massif transferred in the reduction step  $\varepsilon$  from  $P_v$  to  ${}^i P$  over the *taxametric distance*  ${}^\mu s_v^{(\varepsilon)}$ . For  $\varepsilon:=+1$ , the distributions of the corpuscle massif lose more and more their resemblance to the initial excitation pattern  $X(j)$ , which can at best be compensated for (within limits) by the *memory stimulator*.

Due to the unequal distribution of taxametric distances  $s$  between the spatial points  $P$  in  $\mathbb{Z}_{\lambda>0}^{2<N}$ , it is advisable to transfer them to the vertices of  $N$  unit vectors in an orthogonal action space  $\mathbb{Z}_{\sqrt{2}}^N$ . In it, each of the  $N$  nodes is at the vertex of a unit vector  $e$ . Since all unit vectors are perpendicular to each other, there is an identical distance  $\sqrt{2}$  between them. The size of  ${}^\mu d_v^{(\varepsilon)}$  has to be adapted to this distance, realized by multiplying  ${}^\mu \otimes_{d_v^{(\varepsilon)}}$  with the metric calculus  ${}^\mu \kappa_v^{(\varepsilon)}$ .

If in the reduction step  $\varepsilon$  a point in space  $P$  carries a corpuscle massif as charge  $\rho$  at time  $\tau$ , then this charge should have been distributed to the neighboring points in space  $P'$  at a subsequent time  $\tau'$ . Such a process consumes energy and its orientation is described as a vector flow. Vector flows from all points  $P$  in space form a vector field. Thus, the components of the vector field represent a force field at every point in space and in every spatial direction. Force is converted energy along a dedicated path. Assuming that in the reduction step  $\varepsilon$  the spatial point  $P_v$  has a corpuscular charge  $Y_v$ , equivalent to its energy input in  $\varepsilon$ , then a portion  $\Delta Y_v$  is transferred to  ${}^i P$  along a path  $\Delta x_i$ . The required force to be applied is  $\Delta {}^\mu F_v(\tau|\varepsilon)$  [14].

$$\partial_j Y_v \cong \frac{\Delta Y_v}{\Delta x_i} = \Delta {}^\mu F_v(\tau|\varepsilon)$$

The large number of spatial points accommodated in  $\mathbb{Z}_{\sqrt{2}}^N$  requires an extensive variety of paths along which kinetic energy is converted. It is plausible that a large number of forces act against each other - a "mixed situation" which the Jacobian matrix  $\mathfrak{S}_{P_a}^{(m)}$  orders [9]. Its elements are denoted by  $\Delta {}^\mu F_v$ , taken at time  $\tau$  in the reduction step  $\varepsilon$ .

$$\mathfrak{S}_{P_a}^{(m)} = \begin{vmatrix} \Delta {}^1 F_1 & \Delta {}^1 F_2 & \Delta {}^1 F_i & \Delta {}^1 F_v & \Delta {}^1 F_m \\ \Delta {}^2 F_1 & \Delta {}^2 F_2 & \Delta {}^2 F_i & \Delta {}^2 F_v & \Delta {}^2 F_m \\ \Delta {}^i F_1 & \Delta {}^i F_2 & \Delta {}^i F_i & \Delta {}^i F_v & \Delta {}^i F_m \\ \Delta {}^v F_1 & \Delta {}^v F_2 & \Delta {}^v F_i & \Delta {}^v F_v & \Delta {}^v F_m \\ \Delta {}^m F_1 & \Delta {}^m F_2 & \Delta {}^m F_i & \Delta {}^m F_v & \Delta {}^m F_m \end{vmatrix}$$

From the signed difference  $[\mathfrak{S}_{P_a}^{(m)}]^T - \mathfrak{S}_{P_a}^{(m)} = \Delta \mathfrak{S}_{P_a}^{(m)}$ , multiplied with the elements by the signature matrix

$${}^{(m)} Sg = P \parallel sg_{k,i,v} \parallel_{(m,m)}$$

under

$$sg_{k,i,v} = \begin{cases} 0 & \forall (k=i) \vee (k=v) \vee i \geq v \\ \sigma(k-i)\sigma(k-v) & \text{sonst} \end{cases}$$

$$\text{für } \sigma(k-x) = \begin{cases} +1 \text{ für } k > x \\ 0 \text{ für } k = x \\ -1 \text{ für } k < x \end{cases}$$

the *vortex strengths*  $w$  of the  $N$  space points  $P$  result in  $\mathbb{Z}_{\sqrt{2}}^N$ . The elements  $sg$  corresponds to the permutation symbol according to *Tullio Levi-Civita (Levi-Civita symbol* [15]).

The components of the rotor of a flux vector  ${}^{P_v} a(\tau|\varepsilon) = \sum_{\mu=1}^m {}^{P_v} Y_\mu e_\mu$  in  $R^m$  are the vorticity  $w_1(P_v), \dots, w_{v-1}(P_v), w_{v+1}(P_v), \dots, w_m(P_v)$ , oriented in the direction of the unit vectors  $e_{1\dots n-1, n+1\dots m}$ .

$$\text{rot}({}^{P_v} a(\tau|\varepsilon)) = \sum_{\substack{k=1 \\ k \neq v}}^m w_k(P_v) e_k$$

Figure 12 shows the planar  $X''(j_1, j_2)$  and linear  $X''(j)$  reconstruction of the initial excitation pattern  $X$  (Figure 6), projected into a volatile with memory stimulator, next to it the reconstruction of  $X$  over 121 vortex strengths  $w$  in linear representation  $w(j)$  with  $j=1\dots 121$ . Below  $\lambda=1.0$  (*consistency*), the excitation pattern  $X$  is completely reconstructed due to the exclusion of lesion-related losses.

If the consistency is reduced to (only)  $\lambda=0.935$ , which corresponds to a removal of 1060 direct connections in the network and simulates a moderate age-related loss of synaptic contact points, the ratios change significantly. Figure 13 shows the consequences for different memory depths  $\eta$  with isometric and rotation-based reconstruction  $X''(j)$  of  $X(j)$ .

$\lambda=1,0$

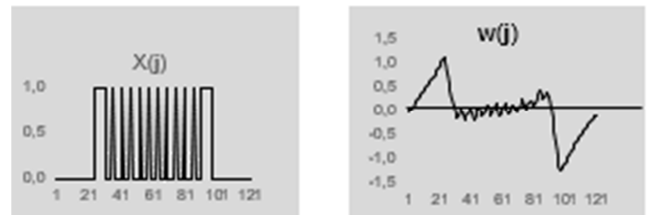


**Figure 12.** Initial excitation pattern  $X$  in a planar  $X(j_1, j_2)$  representation and as an ordered sequence  $X(j)$  of excitation elements, on the right the ordered distribution of the vortex strengths  $w(j)$  over all  $N$  nodes.

With decreasing memory depth  $\eta$  the ability of the population to reconstruct, simulated by the memory stimulator of the volatile network, generally evaporates. This drop is measured by the correlation coefficient  $r(X(j); X''(j))$  [11].

If  $X''(j)$  is the result of an isometric reconstruction of  $X(j)$ , then in the reduction step  $\varepsilon=1,000$  for  $0.8 < \eta < 1,0$  the partial drop in the correlation coefficient  $r$  ends at 0.9 (Figure 10). From the reduction step  $\varepsilon=10,000$  on isometric reconstruction with a memory depth of (only)  $\eta=0,9$  no correlation  $r > 0.9$  can be established. From  $\varepsilon=60,500$ , this also applies to the (maximum) memory depth  $\eta=1,0$ . If, on the other hand,  $X''(j)$

is the reconstruction of  $X(j)$  on the basis of circulating corpuscular flows, such a limitation does not exist.

Figure 13 illustrates the development of vortex strengths in the nodes of the network. Assuming a fully coupled topology, the strongly emphasized curve reflects the conditions at a consistency rate of  $\lambda=1.0$ , identical for all(!) memory depths  $\eta$ . Decreasing consistency rates  $\lambda$  also form here for different memory depths  $\eta$  a smoothing of the reconstruction  $X''(j)$  compared to  $X(j)$ , now caused by a differentiated flow field that swirls around each node, referred to as *vortex strength*  $w$ .

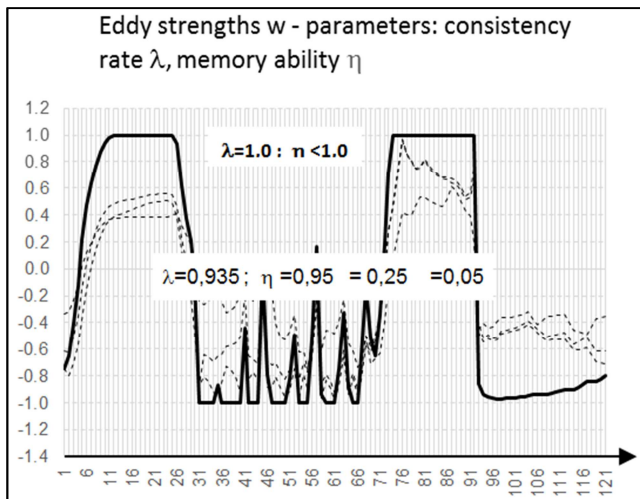


Figure 13. Distribution of vorticity  $w$  in the network of 121 nodes.

It provides information about which Consequence the removal of direct connections between the nodes takes place. To a certain extent, information about whether a reconstruction of the initial excitation pattern is still possible or not. A complete reconstruction for all memory depths  $\eta$  is also given for the parameter set  $\lambda=1.0$  given in Figure 13. Even with a decreasing consistency rate  $\lambda$  and decreasing memory depth  $\eta$ , this ability based on a reconstruction of  $X(j)$  using vortex strengths stands out compared to the isometric reconstruction.

## 4. Conclusion

Isometric reconstructions and reconstructions based on vortex strengths of initial excitation patterns of a neuron population were compared. The prerequisite is that the interactions between the neurons of the population correspond to one and the same discrete functional transformation through the coefficients. On the basis of a functional transformation, different classes of excitation patterns, acoustic, optical, etc., can be related to one another.

With regard to the reconstruction of the excitation pattern, the correlation coefficient  $r(X(j);X''(j))$  is used as a quality criterion. In isometric reconstruction, the congruence of the density distribution of transmitter molecules on the membrane surfaces of the neurons is important. On the other hand, if the correlation coefficient is based on the distribution of vortex strengths in the population, triggered by location-

variable changes in the direction and intensity of the transmitter flows between the neurons, an alternative situation exists.

In principle, the ability of a neuron population to reconstruct depends on its consistency, but also depends, last but not least, on an existing, lost or poorly acquired memory ability. With reference to the previous explanations, the curves in Figures 10 and 3-9 favor the assumption that the memory ability of a neuron population on the basis of vortex strengths, the expression of which is characterized by the direction of transmitter flows of different densities, is superior to the memory ability through isometric reconstruction seems to be. Under this condition, the assumption of engrams for the storage of memory contents proves to be close to reality, the penetration of which also provides information processing.

From the point of view of systems theory, the extracorporeal evaluation of engrams on the basis of evoked potentials would be a starting point for the non-invasive perception of pre-diagnostic symptoms of neurodegenerative diseases [16].

## Acknowledgements

Think former colleague at the TU Dresden, Mr. Dipl.-Inf. Wagner and Mr. Dipl.-Inf. Mr. Lehmann, thank you very much for your commitment in creating the simulation program for an volatile topology. Last but not least, I would like to thank my wife for her patience and tolerance in dealing with the subject.

## References

- [1] Hubel, D. H.; Wiesel, T. N.: Receptive field of single neurons in the cat's Striate Cortex. J. Physiol. (1959) 148, S. 589.
- [2] Semon, R.: Mnemic Psychology. London: GEORGE ALLEN & UNWIND LTD. 1923.
- [3] Gerstner, W.; Kistler, W. et al.: Neuronal dynamics: from single neurons to networks and models of cognition. Cambridge: Cambridge University Press, 2014.
- [4] Nötzel, M.; Hermann, A. et al.: Measuring physical properties of living neurons: a novel Approach to study neurodegeneration. Klinik und Poliklinik für Neurologie Dresden, 2021.
- [5] Sperry R. W.: Cerebral organization and behavior. Science 133 (1961), S. 1749–1757.
- [6] Morbus Alzheimer – Mitochondrien in Zellen blockiert Nach einer Mitteilung der Albert-Ludwigs-Universität Freiburg Aus: Fortschritte Neurologie Psychiatrie 2014.
- [7] Ozansoy, M; Başak, A.: A Tauopathies: A Distinct Class of Neurodegenerative Diseases. Walter de Gruyter GmbH, 2007.
- [8] Eva-Maria und Eckhard Mandelkow: 2013 Khalid Iqbal Lifetime Achievement Award. Alzheimer's Association International Conference (AAIC 2013) Boston (USA).

- [9] Debnath, L; Bhatta, D: Integral transforms and their applications. Chapman & Hall/CRC, 2007 ISBN 1584885750; 9781584885757.
- [10] Jitsev, E.: On the self-organization of a hierarchical memory for compositional object representation in the visual cortex. Publication Server of Goethe University Frankfurt am Main, 2011.
- [11] Jockel, S.: Crossmodally Learning and Prediction of Autobiographical Episodic Experiences using a Sparse Distributed Memory. Staats- und Universitätsbibliothek Hamburg Carl von Ossietzky, 2009.
- [12] Hainmueller, T.; Bartos M.: The hippocampus converts dynamic entorhinal inputs into stable spatial maps Institute for Physiology I, University of Freiburg, Medical Faculty, Freiburg.
- [13] Wagner, Th.; Lehmann, M.: Analyse und Synthese Massiv Paralleler Systeme Technische Universität Dresden, Fakultät Informatik. 2007.
- [14] Dallmann, H.; Elster K.-H.: Einführung in die Höhere Mathematik 3. Friedrich Vieweg & Sohn Braunschweig/Wiesbaden, 1983. ISBN 3-528-03586-2.
- [15] Riley, K. F.; Hobson, M. P. et al.: Mathematical Methods for Physics and Engineering. Cambridge University Press ISBN 978-0-521-86153-3.
- [16] Haußmann, R.; Bauer, M. et al.: Prädikation von Neurodegeneration in der multidimensionalen Demenzdiagnostik. Klinik und Poliklinik für Psychiatrie und Psychotherapie Dresden, Klinik und Poliklinik für Psychiatrie und Psychotherapie Dresden, 2020.